# Conformational Studies by Dynamic Nuclear Magnetic Resonance. 59.[1] Stereodynamics of Conformational Enantiomers in the Atropisomers of Hindered Naphthylcarbinols

Daniele Casarini,* Lodovico Lunazzi, and Andrea Mazzanti[2]

*Department of Organic Chemistry "A. Mangini", University of Bologna, Risorgimento, 4, Bologna 40136, Italy*

*Received January 22, 1997*[⊗]

Naphthyldialkylmethanols ArRR′COH (Ar = 1-naphthyl or 1-naphthyl-2-methyl) exist as a pair of atropisomers created by the restricted rotation about the Ar−COH bond. They can be detected by low-temperature NMR spectroscopy but can also be separated as stable compounds at room temperature if both the alkyl substituents are bulky *tert*-butyl groups (one such example is provided by compound **1**, R = R′ = Bu$^t$ with Ar = 1-naphthyl). The free energies of activation ($\Delta G^{\ddagger}$) for the interconversion of these atropisomers were found to vary between 7.6 kcal mol$^{-1}$ (as in **7**, R = R′ = Me, Ar = 1-naphthyl-2-methyl) and 32.9 kcal mol$^{-1}$ (as in **1**). The *syn*-periplanar (sp) or *anti*-periplanar (ap) structures were assigned either by means of difference NOE experiments or by taking advantage of the H-8 chemical shifts which are vastly different in the two atropisomers. Depending on the substituents the more stable species at the equilibrium can be either the sp or the ap atropisomer. When R = R′ = Pr$^i$ and R = R′ = Et (respectively **2** and **3** if Ar = 1-naphthyl), the sp atropisomers adopt an asymmetric conformation, thus creating a pair of conformational enantiomers which interchange by rotating the isopropyl or the ethyl groups about the appropriate sp$^3$−sp$^3$ bonds, with $\Delta G^{\ddagger}$ values of 7.2 and 6.1 kcal mol$^{-1}$, respectively. On the contrary the corresponding **3**-ap and **2**-ap atropisomers adopt a symmetric (meso) conformation, as predicted by molecular mechanics calculations. In the case of R = Pr$^i$, R′ = Et, and Ar = 1-naphthyl (**10**-sp atropisomer), two asymmetric conformers were found to be appreciably populated (ratio 9:1 at −135 °C).

## Introduction

Restricted rotation about the sp$^2$−sp$^3$ Ar−COH bond in carbinols of the type Ar−C(Bu$^t$)$_2$OH (Ar being the 4-methoxyphenyl moiety) was first reported[3a] by Sternhell and co-workers. They also identified the presence of two *syn* and *anti* conformers[3] when the Ar group (e.g., Ar = 3,4-dimethoxyphenyl) bore substituents in positions which destroyed the 2-fold Ar−COH symmetry axis of the phenyl (or of the para-substituted phenyl groups). The barrier for the Ar−COH rotation was measured (about 20 kcal mol$^{-1}$) by variable temperature $^1$H NMR spectroscopy.[3] When less hindered carbinols (e.g., Ar−CRBu$^t$OH, with R = H, Me, Et, Pr$^i$) were investigated, the interconversion barriers were found, not unexpectedly, considerably lower ($\Delta G^{\ddagger}$ in the range 8.7−13.0 kcal mol$^{-1}$).[4] Subsequently Lomas and Dubois[5,6] were able to isolate the rotational isomers (atropisomers[7]) of Ar−C(Bu$^t$)$_2$OH, by making use of a more hindered derivative (i.e., the one with Ar = *o*-tolyl) which has a significantly larger interconversion barrier (25.9 kcal mol$^{-1}$). X-ray diffraction of the thermodynamically more stable atropisomer of a very similar compound (i.e., that having Ar = 2-methyl-4-methoxyphenyl) indicated that a *syn*-periplanar (sp) structure is adopted. The OH group, in fact, points toward the *o*-methyl substituent, with the C−OH bond lying, in practice, on the same plane of the aromatic ring, the corresponding dihedral angle deviating only by 11.6° from a perfect coplanarity.[6] In solution, of course, a low-barrier libration process of ±11.6° would cause this plane to become a dynamic plane of symmetry. Atropisomers of this type, with even larger interconversion barriers, were observed for adamantyl (Ad) derivatives such as Ar−C(Ad)$_2$OH and Ar−CBu$^t$AdOH, Ar being again the *o*-tolyl group.[8,9] In addition to the mentioned rotational process about the sp$^2$−sp$^3$ bond, a second rotational process was detected about the sp$^3$−sp$^3$ Bu$^t$−COH bonds in Ar−C(Bu$^t$)$_2$OH (Ar = *o*-tolyl). The barriers for the rotation of the *tert*-butyl groups are not equal in the two atropisomers, that of the *syn*-periplanar (more stable) being higher than that for the *anti*-periplanar ($\Delta G^{\ddagger}$ = 10.3 and 9.3 kcal mol$^{-1}$, respectively).[10] Carbinols bearing the 1-naphthyl substituent should also display similar conformational properties, and an investigation on such derivatives (**1**−**4**) is the subject of the present study.

So far this type of atropisomerism was only observed in the case of highly hindered carbinols, having a *tert*-butyl or an adamantyl group as one of the substituents R (there is also a case where both the substituents were isopropyl groups[4]): compounds **3** and **4** (R = Et and Me, respectively) will show that this phenomenon is amenable to observation also in less hindered systems. More

[⊗] Abstract published in *Advance ACS Abstracts,* April 1, 1997.

(1) For part 58, see: Lunazzi, L.; Mazzanti, A.; Spagnolo, P.; Degl' Innocenti, A. *J. Org. Chem.* **1997**, *62*, 2263.

(2) In partial fulfillment of the requirements for the Ph.D. degree in Chemical Sciences, University of Bologna.

(3) (a) Newsoroff, G. P.; Sternhell, S. *Tetrahedron Lett.* **1967**, 2539. (b) Landman, D.; Newsoroff, G. P.; Sternhell, S. *Aust. J. Chem.* **1972**, *25*, 109.

(4) Baas, J. M. A.; van der Toorn, J. M.; Wepster, B. M. *Recl. Trav. Chim. Pays-Bas* **1974**, *93*, 173.

(5) Lomas, J. S.; Dubois, J.-E. *J. Org. Chem.* **1976**, *41*, 3033.

(6) Lomas, J. S.; Luong, P. K.; Dubois, J.-E. *J. Org. Chem.* **1977**, *42*, 3395.

(7) This definition is taken from ref 5 and 6. (See also: Ikeda, Y.; Kato, N.; Mori, A.; Takeshita, M. *Magn. Reson. Chem.* **1992**, *30*, 476. Zoltewicz, J. A.; Maier, N. M.; Fabian, W. M. *Tetrahedron* **1996**, *52*, 8703.)

(8) Lomas, J. S.; Dubois, J.-E. *Tetrahedron* **1981**, *37*, 2273.

(9) Lomas, J. S.; Anderson, J. E. *J. Org. Chem.* **1995**, *60*, 3246.

(10) Tiffon, B.; Lomas, J. S. *Org. Magn. Reson.* **1984**, *22*, 29.

S0022-3263(97)00113-8 CCC: $14.00 

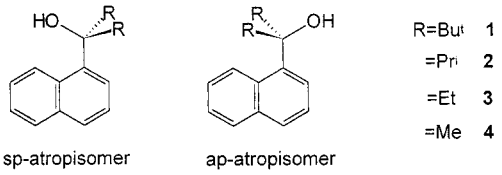


importantly, derivatives **2** and **3** are suited to investigate a hitherto unreported feature in this type of carbinols, i.e., the possible existence of conformational enantiomers which, in principle, can be created by the restricted rotation of the ethyl or isopropyl substituents: these moieties lack, in fact, the local symmetric 3-fold rotational axis of the *tert*-butyl (or methyl) group of **1** (or **4**).

## Results and Discussion

The reaction employed (see the Experimental Section) to obtain carbinol **1** (R = *tert*-butyl) yields two compounds (i.e., the two expected atropisomers), one being a liquid, the other a solid. Although in the reaction mixture the solid is present in a larger amount with respect to the liquid, thermal equilibration (carried out at 116 °C in DMSO) indicates, on the contrary, that the solid atropisomer is thermodynamically less stable, its proportion at the equilibrium being about 2%. Obviously the predominance of the solid atropisomer in the synthetic process is the result of a kinetically controlled reaction. The rate constant for transforming the more stable into the less stable atropisomer was found to be $2.78\ 10^{-6}\ s^{-1}$, which corresponds (at 116 °C) to a free energy of activation ($\Delta G^{\ddagger}$) of 32.9 kcal $mol^{-1}$ (the rate constant for the reverse process is $1.36\ 10^{-4}\ s^{-1}$; hence a $\Delta G^{\ddagger} = 29.9$ kcal $mol^{-1}$). Of course the two atropisomers have different $^{13}C$ and $^{1}H$ NMR spectra; in particular, the H-8 signal of the liquid appears at much lower field (9.50 ppm) than that of the solid compound (8.60 ppm).

Structural assignment of the two atropisomers of **1** was achieved by difference NOE experiments. Irradiation of the OH line enhances the H-2 but not the H-8 signal of the solid, whereas the opposite occurs in the liquid atropisomer. In addition, irradiation of the *tert*-butyl line enhances the H-8 much more than the H-2 signal in the solid, while the opposite trend is observed in the liquid atropisomer (Table 1). Thus the *syn*-periplanar (sp) structure can be unambiguously assigned to the more stable (liquid) and the *anti*-periplanar (ap) structure to the less stable (solid) atropisomer. The large low-field shift of the H-8 signal in the NMR spectrum of atropisomer **1**-sp can be understood on the basis of an intramolecular hydrogen bonding between the oxygen and the H-8 atom (this being facilitated by the possibile existence of a nearly planar six-membered ring), a feature which is known to move significantly downfield the chemical shifts of the hydrogens involved. This finding can thus be used as a diagnostic tool for assigning the sp or ap structures in other naphthylcarbinols of this series.

In the case of **2** (R = isopropyl) the two atropisomers could not be separated, but their individual NMR spectra were observed at low temperature, their signals having a 78:22 ratio in $CD_2Cl_2$. In Figure 1 (left) the $^{13}C$ NMR spectra of the methyl signals of **2** are displayed as a function of temperature. At −20 °C two widely separated lines for the minor and two closely spaced lines for the major atropisomer are visible. These lines broaden and coalesce at higher temperatures, eventually displaying

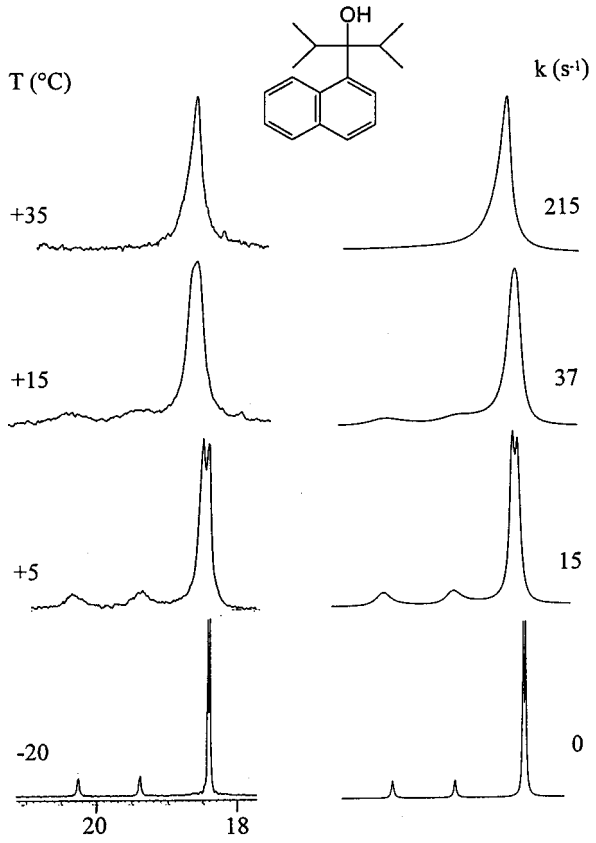


**Figure 1.** (Left) Experimental isopropyl methyl signals of **2** ($^{13}C$ NMR, 75.5 MHz) as a function of temperature in $CD_2Cl_2$ showing, at −20 °C, a weaker pair of signals (downfield) for the ap and a more intense pair of signals (upfield) for the sp atropisomer. (Right) Computer simulation obtained with the rate constants indicated.

**Table 1. NOE Effects Observed in the Two Atropisomers of 1 (in $CDCl_3$ at 22 °C) and the Two Atropisomers of 2 (in $CD_2Cl_2$ at −70 °C)**

| | | observed NOE (%) | |
|---|---|---|---|
| atropisomer | satd signal | H-2 | H-8 |
| **1**-sp | OH | | 5 |
| | $Me_3$ | 25 | 10 |
| **1**-ap | OH | 8 | |
| | $Me_3$ | 6 | 18 |
| **2**-sp | OH | | 12 |
| | *CH*($Me_2$) | 23 | |
| **2**-ap | OH | 11 | |
| | *CH*($Me_2$) | | 30 |

a unique pair of lines above 50 °C (this is not shown in the picture because a solvent with a higher boiling point than that of $CD_2Cl_2$ had to be used). The methyl groups within each of the two isopropyl substituents are, in fact, diastereotopic since the local plane bisecting the Me−CH−Me angle is not coincident with the plane of symmetry for the whole molecule.[11] From the rate constants needed to achieve the computer simulation (Figure 1, right), the free energy of activation ($\Delta G^{\ddagger} = 14.9$ kcal $mol^{-1}$) for the exchange between the major (**2**-sp) and the minor (**2**-ap) atropisomer was obtained (Table 2). The $\Delta G^{\ddagger}$ values were found, within the errors (±0.2 kcal $mol^{-1}$), independent of temperature, as often occurs in the dynamics of intramolecular processes; thus, the free energies of activation were considered throughout a

(11) (a) Mislow, K.; Raban, M. *Topics Stereochem.* **1967**, *1*, 1. (b) Jennings, W. B. *Chem. Rev.* **1975**, *75*, 307. (c) Eliel, E. L. *J. Chem. Educ.* **1980**, *57*, 52.

**Table 2. Ratio of the sp and ap Atropisomers at Equilibrium and Free Energies of Activation ($\Delta G^{\ddagger}$, kcal mol$^{-1}$) for Their Interconversion in Derivatives 1−8, 10 and 11**

| compd | sp:ap ratio[a] | $\Delta G^{\ddagger}$ [b] | $T$ range (°C)[c] | solvent |
|---|---|---|---|---|
| **1** | 98:2 (116) | 32.9 | 116 | DMSO-$d_6$ |
| **2** | 78:22 (−20) | 14.9 | 6−38 | $CD_2Cl_2$ |
| **3** | 54:46 (−83) | 9.7 | −67 to −62 | $CD_2Cl_2$ |
| **4** | 92:8 (−133) | 8.4 | −109 | $Me_2O$ |
| **5** | 15:85 (23) | 17.2 | 70−100 | DMSO-$d_6$ |
| **6** | 37:63 (−95) | 10.0 | −75 to −60 | $CD_2Cl_2$ |
| **7** | 30:70 (−130) | 7.6 | −125 to −115 | $Me_2O$ |
| **8** | 90:10 (−15) | 16.4 | 30−75 | $C_2Cl_4$ |
| **10** | 30:70 (−62) | 12.3 | −38 to −28 | $CD_2Cl_2$ |
| **11** | 80:20 (−98) | 9.7 | −83 to −62 | $CD_2Cl_2$ |

[a] In parentheses is the temperature (°C) at which the ratio was measured. [b] Barriers required to interconvert the *more* stable into the *less* stable atropisomer. [c] Range where line shape simulation was performed (except for **1**, see text).

reliable measure of the interconversion barrier. The sp structure was assigned to the major atropisomer because it exhibits the H-8 signals at a field much lower (9.45 ppm) than the minor one (8.27 ppm). Such a conclusion was checked again by NOE measurements, which were carried out at −70 °C in order to avoid possible saturation transfer effects (from the measured $\Delta G^{\ddagger}$ value the exchange rate between the two atropisomers was computed to be too slow at that temperature to interfere with the NOE effect). As shown in Figure 2, simultaneous irradiation of the two OH signals enhances only the H-8 signal of the major (sp) and the H-2 signal of the minor (ap) atropisomer. Conversely, simultaneous irradiation of the two CH signals of the isopropyl groups only enhances the H-8 signal of the minor (ap) and the H-2 signal of the major (sp) atropisomer (Table 1).

Analogous dynamic NMR spectra were observed for the ethyl and methyl derivatives (**3** and **4**, respectively) where the lower steric hindrance of these alkyl substituents made the corresponding barriers (Table 2) even smaller ($\Delta G^{\ddagger}$ = 9.7 and 8.4 kcal mol$^{-1}$, respectively). The amount of the sp atropisomer at the equilibrium decreases regularly along the series R = Bu$^t$, Pr$^i$, Et (i.e., 98%, 78%, and 54% for **1**−**3**, respectively). Strangely enough its proportion, on the contrary, increases when R = methyl (it is 92% in **4**, as shown in Table 2). Although a simple explanation for such an irregular trend is not available, MM calculations[12a] indicate indeed that the amount of sp atropisomer in **4** is similar to that of **1**, and both are larger than the corresponding amounts computed in the case of **2** and **3**.

Introduction of a methyl group in position 2 of the naphthalene ring modifies the steric requirements, thus altering both the atropisomer ratio and the corresponding interconversion barriers. The derivatives investigated (**5**−**7**) are shown below. Unfortunately we have been unable to prepare the analogous derivative having R = *tert*-butyl, most likely owing to an exceedingly severe steric hindrance.

In **5**−**7** the two atropisomers were detected by low-temperature NMR, but contrary to what was observed in **1**−**4**, the ap was found more stable, in all three cases, than the sp atropisomer. This assignment was based on the values of the corresponding H-8 shifts, although in the case of **5** this was further confirmed by the large, reciprocal NOE effect observed between the H-8 and CH isopropyl signals of the major atropisomer at −25 °C.

In addition to reversing the ratio of the atropisomers, the methyl group in position 2 also modifies the interconversion barriers by acting in two possible manners, i.e., reducing mainly either the stability of the ground state or that of the rotational transition state. In the case of R = isopropyl (**5**) the second possibility dominates;

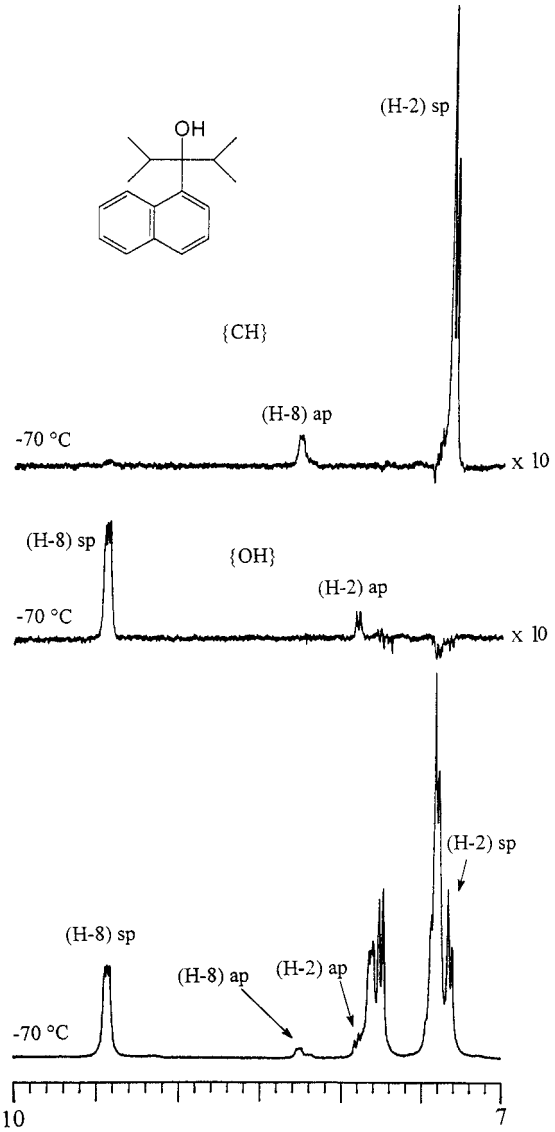


**Figure 2.** Difference NOE spectra (in $CD_2Cl_2$ at 300 MHz) of the aromatic region of **2** at −70 °C. Simultaneous irradiation of the isopropyl methine signals of both atropisomers enhances the H-8 signal of the ap (minor) and the H-2 signal of the sp (major) atropisomer (top trace). On the contrary simultaneous irradiation of the OH signals of both atropisomers enhances the H-8 signals of the sp (major) and the H-2 signals of the ap (minor) atropisomer (middle trace). The vertical scales of the NOE spectra are amplified by a factor of 10 with respect to that of the control spectrum (bottom trace).

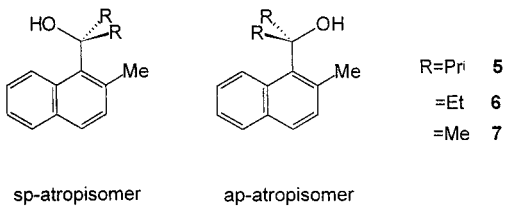


(12) (a) The MMX force field (as implemented in the program PC Model, Serena Software, Bloomington, IN) has been employed. (b) These calculations indicate that the plane containing the C−OH bond is tilted out of the naphthalene plane by 10° in **1**-sp and 7° in **1**-ap; cf. the X-ray value of 11.6° reported in ref 6 for a similar compound.

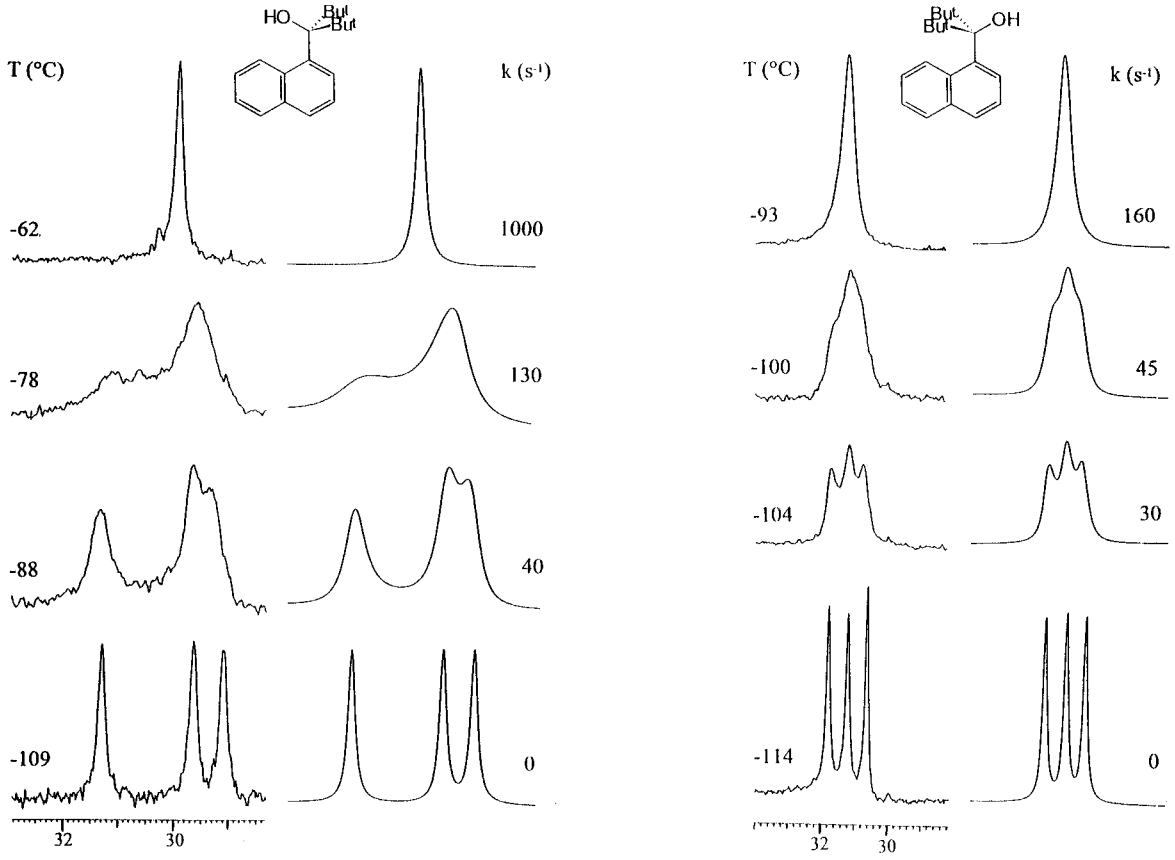


**Figure 3.** (Left) Experimental and computer-simulated methyl signals ($^{13}$C NMR, 75.5 MHz) of atropisomer **1**-sp as a function of temperature in $Me_2O$. (Right) Analogous spectra for the atropisomer **1**-ap in the same conditions.

thus the barrier becomes *larger* than that of the unsubstituted analog **2** ($\Delta G^{\ddagger}$ = 17.2 vs 14.9 kcal mol$^{-1}$). On the contrary in the less hindered derivative **7** (R = methyl) the first situation prevails, thus making the corresponding barrier *lower* than that of the unsubstituted analog **4** ($\Delta G^{\ddagger}$ = 7.6 vs 8.4 kcal mol$^{-1}$). In the case of **6** (R = Et) the two effects are almost equally balanced, thus leaving the barrier *equal*, within the errors (±0.2 kcal mol$^{-1}$), to that of the unsubstituted analog **3** ($\Delta G^{\ddagger}$ = 10.0 and 9.7 kcal mol$^{-1}$, respectively). The results are collected in Table 2.

A second motion, which occurs at much lower temperature than required for interconverting the two atropisomers, has been observed in **1**. The $^{13}$C methyl signal of each atropisomer (**1**-sp and **1**-ap) splits into three lines with a 1:1:1 relative intensity (Figure 3). By analogy with previous results,[10] this feature should be attributed to the restricted rotation of the *tert*-butyl moieties, which leads to a situation where the methyl groups occupy three different environments. The barrier for such a process, determined by computer line shape simulation (Figure 3), is higher in the more stable (**1**-sp, liquid) than in the less stable (**1**-ap, solid) atropisomer, the $\Delta G^{\ddagger}$ values being respectively 9.3 and 8.6 kcal mol$^{-1}$ (Table 3). The $^{13}$C NMR spectra also indicate that in both atropisomers the naphthalene ring is still a molecular plane of symmetry, even when the rotation of the two *tert*-butyl groups is slow. The six methyl groups display, in fact, only three lines, and the two $CMe_3$ quaternary carbons display a single line. This requires that the two *tert*-butyl moieties remain indistinguishable, even at such a low temperature. However, as suggested by common sense, the MM calculations predict[12] that the two *tert*-butyl groups are not eclipsed but somehow staggered, with a reciprocal dihedral angle of about 30°. Clearly such an arrangement would produce six $^{13}$C methyl lines (and two quaternary carbon lines) for each atropisomer, contrary to the experimental evidence. Thus a 30° libration process must still be fast, in order to exchange the positions of the methyl groups on one side of the naphthalene ring with the corresponding ones on the opposite side. The barrier for such a motion must be much lower than that for the 360° rotation which exchanges the three methyl groups *within* each of the two *tert*-butyl moieties and thus is NMR invisible.

**Table 3. Barriers ($\Delta G^{\ddagger}$, kcal mol$^{-1}$) for the Rotational Process of Alkyl Groups (R) about the R−COH Bond**

| compd | R group | $\Delta G^{\ddagger}$ | *T* range (°C)[a] | solvent |
|---|---|---|---|---|
| **1**-sp | Bu$^t$ | 9.3 | −88 to −78 | $Me_2O$ |
| **1**-ap | Bu$^t$ | 8.6 | −104 to −93 | $Me_2O$ |
| **2**-sp | Pr$^i$ | 7.2 | −125 to −120 | $Me_2O/CD_2Cl_2$ |
| **3**-sp | Et | 6.1 | −140 | $CHF_2Cl/Me_2O$ |
| **8**-sp | Bu$^t$ | 7.3 | −125 to −120 | $Me_2O$ |
| **10**-sp | Pr$^i$ | 7.6 | −110 | $CHF_2Cl/Me_2O/CD_3OD$ |

[a] Range where line shape simulation was performed.

The relatively high barriers[13] for the rotation of the *tert*-butyl groups in **1**-sp and **1**-ap are a consequence of the reciprocal interactions between two such substituents. If one of them is replaced by a less bulky substituent (e.g., a methyl group) the barrier should become lower. To check this point we synthesized derivative **8** which displays, as usual, the spectra of the sp and ap atropisomers at low temperature.

The more stable atropisomer (about 90% at −15 °C) is **8**-sp, which interconverts into **8**-ap with a $\Delta G^{\ddagger}$ = 16.4

(13) Anderson, J. E. In *The Chemistry of Alkanes and Cycloalkanes*; Patai, S., Rappoport, Z., Eds.; Wiley: London, 1992; Chapter 3, p 95.

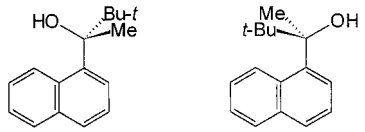


sp-atropisomer ap-atropisomer **8**

kcal mol$^{-1}$. On further lowering the temperature the $^{13}$C single line corresponding to the three methyl groups of the *tert*-butyl moiety of atropisomer **8**-sp broadens and eventually splits (at −135 °C) into three lines.[14] The corresponding rotational barrier ($\Delta G^{\ddagger}$ = 7.3 kcal mol$^{-1}$) was found indeed lower (by 2 kcal mol$^{-1}$) than that measured for the *tert*-butyl rotation in the more hindered **1**-sp derivative (the corresponding barrier for the **8**-ap atropisomer could not be measured since at very low temperatures the weaker signal of its *tert*-butyl group is overlapped by those of the major atropisomer).

As anticipated in the Introduction, the substituents lacking the symmetric local 3-fold rotational axis of the *tert*-butyl group might produce conformers deprived of any element of symmetry (i.e., conformational enantiomers). For instance, in each of the two atropisomers of **2** (R = Pr$^{i}$) and **3** (R = Et), the two Pr$^{i}$−COH or the two Et−COH bonds might be regarded as a pair of stereogenic axes,[15] each being able to generate a chiral situation which would therefore lead either to meso or to racemic stereolabile diastereoisomers (conformers). As a consequence when the rotation of the isopropyl groups in **2** or of the ethyl groups in **3** is slow, each atropisomer of **2** and **3** might adopt conformations which retain a plane of symmetry (meso) or conformations which lose any element of symmetry (racemic). Molecular mechanics calculations predict that both situations should be observable, depending on which atropisomer is examined, and these predictions were, apparently, verified by our experiments.

In the case of the *syn*-periplanar atropisomer of **2** (R = Pr$^{i}$), the most stable conformer was computed to be the one where the CH bonds of the two isopropyl groups adopt a dihedral angle of about 110° (Chart 1, left). In this way the two isopropyl methyl groups avoid having an unfavorable 1,3-parallel interaction. Such an arrangement entails the existence of an asymmetric, thus chiral, structure yielding a pair of conformational enantiomers (i.e., a racemic conformer), and the $^{13}$C NMR spectrum of **2**-sp should therefore display two signals for the two diastereotopic isopropyl CH carbons (and, for the same reason, four signals for the diastereotopic methyl groups) when the rotation is made sufficiently slow at appropriate low temperature.

**Chart 1. Schematic Representation[16] of the Most Stable Conformers of Atropisomer 2-sp (chiral, left) and Atropisomer 2-ap (Meso, right)[a]**

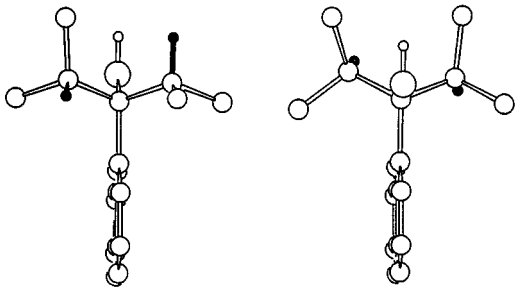

**2**-sp **2**-ap

[a] Only the OH and the CH isopropyl hydrogens (the latter in black) are reported.

The same calculations predict, on the contrary, that in the *anti*-periplanar (**2**-ap) atropisomer the most stable conformation has the two isopropyl CH bonds forming a much smaller dihedral angle than in **2**-sp (i.e., 30° rather than 110°). As shown in Chart 1 (right) the isopropyl methyl groups do have, now, the unfavorable 1,3-parallel interaction, but in **2**-ap this is required to avoid the even more unfavorable interaction of the methyl groups with H-8 of the naphthalene ring. The situation encountered in **2**-ap somehow parallels that of the *tert*-butyl derivatives **1**: here too a low barrier libration process would make equivalent (enantiotopic) the two isopropyl moieties, with the naphthalene ring retained as a dynamic plane of symmetry. Consequently the low-temperature NMR spectrum of **2**-ap should not display any splitting of the $^{13}$C lines when the isopropyl rotation is slow.

The $^{13}$C NMR spectra of **2** seem to agree well with these hypotheses. As shown in Figure 4, where the $^{13}$C signals of isopropyl CH are reported, two closely spaced lines are visible at −93 °C, the one at lower field due to the major (**2**-sp) and that at higher field due to the minor (**2**-ap) atropisomer. The downfield line is already broader than the other and further broadens on lowering the temperature, eventually splitting (at −130 °C) into a pair of equally intense lines, as expected for an asymmetric (chiral) conformation like that in Chart 1 (left). On the contrary, the upfield line of **2**-ap does not undergo exchange broadening, as conceivable for a symmetric (meso) conformation like that in Chart 1 (right). Accordingly, the pair of lines corresponding to the diastereotopic methyl groups of **2**-sp also broadens and subsequently splits into four lines at −135 °C, whereas that of the **2**-ap atropisomer does not.[17] The process which exchanges one conformational enantiomer into the other, by rotating the isopropyl groups of **2**-sp, was found to have a $\Delta G^{\ddagger}$ = 7.2 kcal mol$^{-1}$ (Table 3).

(14) In the isomer of **8** having the MeC(OH)Bu$^{t}$ moiety in position 2 of the naphthalene ring (compound **9**), the $^{13}$C line of the *tert*-butyl methyl group broadens at low temperature (in $Me_2O$) and subsequently splits (at −110 °C) into two, with about a 1:1 ratio. These two groups of lines are due to the spectra of the sp and ap atropisomers, which have almost the same population, owing to the similarity of their steric requirements. In the same temperature range one of these two lines (that at lower field) broadens and splits into three (owing to a restricted *tert*-butyl rotation, with a barrier almost equal to that responsible for the atropisomer interconversion), whereas that at higher field remains unsplit. This different behavior of the two atropismers could be due to a separation of the three methyl $^{13}$C shifts too small to be observed.

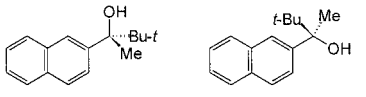


sp-atropisomer ap-atropisomer **9**

(15) (a) Casarini, D.; Foresti, E.; Gasparrini, F.; Lunazzi, L.; Macciantelli, D.; Misiti, D.; Villani, C. *J. Org. Chem.* **1993**, *58*, 5674. (b) Casarini, D.; Lunazzi, L.; Gasparrini, F.; Villani, C.; Cirilli, M.; Gavuzzo, E. *J. Org. Chem.* **1995**, *60*, 97. (c) Casarini, D.; Lunazzi, L.; Alcaro, S.; Gasparrini, F.; Villani, C. *J. Org. Chem.* **1995**, *60*, 5515.

(16) Whereas in the ap atropisomers the MM calculations[12a] indicate that the C−O−H moiety is essentially coplanar with the naphthalene ring, the same calculations indicate that in the sp atropisomers there is a deviation from coplanarity by a small dihedral angle, whose value depends on the molecule investigated. Since the OH moiety experiences, however, a low-barrier libration above and below the naphthalene ring, the plane containing the C−O−H group has been drawn as coplanar also in the case of the sp atropisomers, in order to somehow visualize the consequence of this very fast process.

(17) In practice only one of the two methyl lines of **2**-ap could be monitored down to −135 °C since the other was obscured by one of the four methyl lines of the major atropisomer **2**-sp.

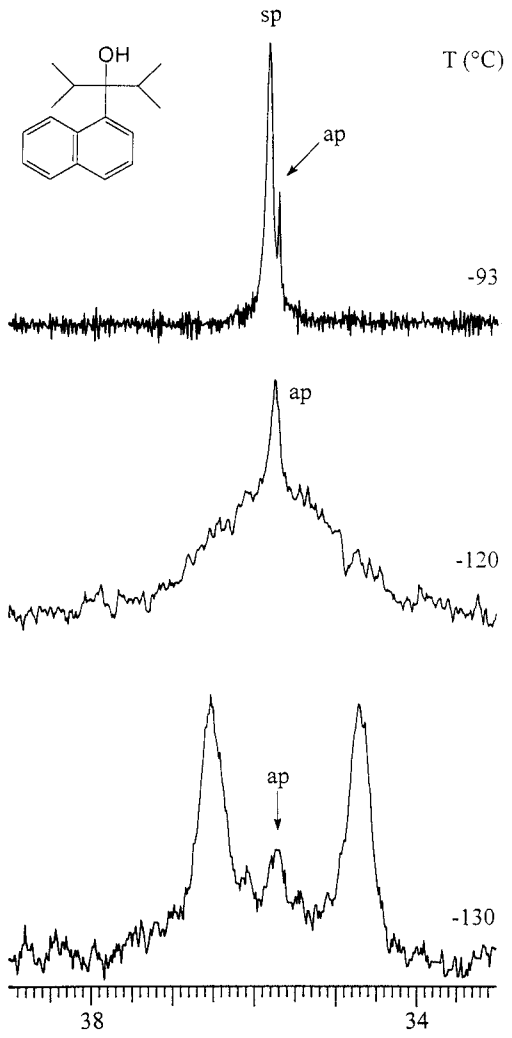


**Figure 4.** Isopropyl methine signals of **2** ($^{13}$C NMR, 75.5 MHz) at different temperatures in $Me_2O/CD_2Cl_2$. At −93 °C two lines are observed for the minor (ap, upfield) and the major (sp, downfield) atropisomer. The latter broadens and splits (at −130 °C) into two equally intense lines, whereas the other does not. This is a consequence of the racemic conformation adopted by **2**-sp and the meso conformation adopted by **2**-ap (Chart 1).

An analogous behavior had been anticipated by MM calculations[12a] for **3** (R = Et), since the conformation having the lowest energy value was predicted to be asymmetric (thus chiral) in **3**-sp, whereas a symmetric (thus meso) conformation was predicted to have the lowest energy value in **3**-ap (Chart 2). Again the experiment apparently supports the theoretical results, as shown in Figure 5 where the $^{13}$C methylene signal of **3** is reported at various temperatures. The single line observed when the two atropisomers are still in rapid exchange (at −41 °C) broadens and splits into two lines (with an accidentally equal intensity in $Me_2O/CHF_2Cl$) at −83 °C. The upfield line of the sp atropisomer[18] then broadens further and eventually splits into two at −146 °C, whereas the downfield line of **3**-ap does not. In **3**-sp the rotational barrier of the ethyl groups, which allows

(18) The upfield $^{13}$C line (in $Me_2O/CHF_2Cl$) is attributed to the **3**-sp atropisomer since in $CD_2Cl_2$ (at −90 °C) this line is more intense than that at lower field and, in the same sample, the H-8 proton signal at 9.07 ppm (which corresponds to the sp atropisomer) is more intense (58%) than that (42%) at 8.08 ppm (corresponding to the ap atropisomer). Apparently in $Me_2O/CHF_2Cl$ the relative stability of atropisomer **3**-ap increases slightly with respect to the situation in $CD_2Cl_2$.

**Chart 2. Schematic Representation[16] of the Most Stable Conformers of Atropisomer 3-sp (Chiral, left) and Atropisomer 3-ap (Meso, right)[a]**

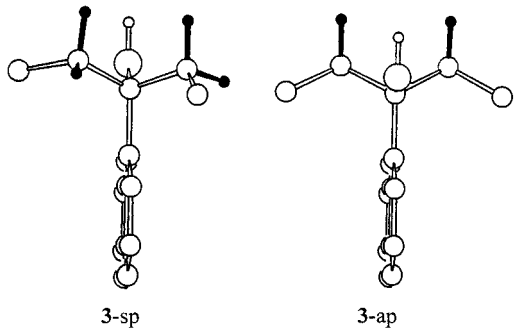


[a] Only the OH and the $CH_2$ hydrogens (the latter in black) are reported.

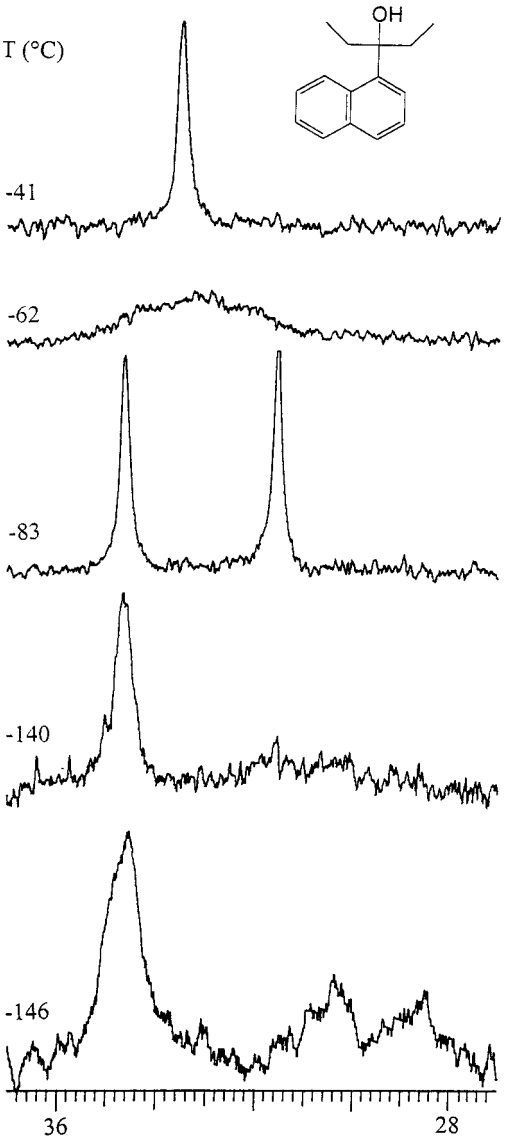


**Figure 5.** Methylene signal of **3** ($^{13}$C NMR, 75.5 MHz) as a function of temperature in $Me_2O/CHF_2Cl$. The single line observed at −41 °C broadens and subsequently splits (−83 °C) into a pair of lines, with an accidentally equal intensity (see ref 18), corresponding to the **3**-ap (downfield) and the **3**-sp (upfield) atropisomer, respectively. The latter further broadens and eventually splits (at −146 °C) into two lines, whereas the other does not. This is because **3**-sp adopts the racemic and **3**-ap the meso conformation shown in Chart 2.

one conformational enantiomer to exchange into the other, was found to have a $\Delta G^{\ddagger} = 6.1$ kcal mol$^{-1}$ (Table 3).[19]

Surprisingly, the corresponding derivatives with a methyl group in position 2 (i.e., **5**, R = Pr$^{i}$; **6**, R = Et) do not display the effects due to R−COH rotational processes in either of the two atropisomers. This might depend upon a rotational barrier of the isopropyl and ethyl moities too low to be detected by NMR. However this seems quite unlikely, as bulkier compounds of this type should experience an even higher hindrance to rotation. MM calculations suggest an alternative explanation for the absence of such an effect. In both atropisomers of **5** and **6** the conformation having the lowest computed energy turns out to be symmetric (meso) in that both **5**-sp and **6**-sp maintain the naphthalene ring as a plane of symmetry, as do **5**-ap and **6**-ap (this behavior, therefore, differs from that of the less hindered analogs **2** and **3** where the sp atropisomers adopt an asymmetric conformation). Thus, if these calculations have to be trusted, the absence of line-broadening effects in **5** and **6** is accounted for by the conservation of the molecular symmetry.

The low-temperature NMR spectra of **2** and **3** show that only a single conformation, respectively asymmetric for the sp and symmetric for the ap atropisomers, is observed although, in principle, more than one conformation (either symmetric or asymmetric) might have been populated. In order to verify whether such a hypothetical situation (i.e., the simultaneous presence of two or more conformers) can, in practice, take place, we further dissymmetrized these compounds, by preparing derivatives **10** and **11**. Here we have a configurationally stable

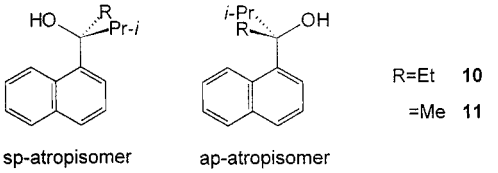


chiral center (i.e., the carbon atom bonded to OH) which might couple its chirality with the second source of chirality created, at low temperature, by the stereogenic conformational axis[15] corresponding to the Pr$^{i}$−COH bond. As two sources of chirality are now available, two stereolabile diastereoisomers (conformers) might become observable.

In the case of **11** (R = Me) the experiment did not fulfill such an expectation since both atropisomers **11**-sp (more stable) and **11**-ap (less stable) displayed a spectrum due to a single rotational conformer, even at −140 °C. Only the interconversion barrier between the two atropisomers could thus be measured (Table 2), and its value ($\Delta G^{\ddagger} =$ 9.7 kcal mol$^{-1}$) was found, as conceivable, intermediate between those of the bulkier derivative **2** (where both the R groups are isopropyl) and of the less crowded derivative **4** (where both the R groups are methyl). MM calculations[12a] account for the presence of a single rotational conformer by showing that in both atropisomers **11**-sp and **11**-ap the most stable conformer has an energy substantially lower than that of the next stable conformer differing by the position of the isopropyl group (the computed energy separation being respectively 1.2 and 3.1 kcal mol$^{-1}$).

**Chart 3. Schematic Representation[16] of the Two Most Stable Conformers (left and center) of Atropisomer 10-sp[a]**

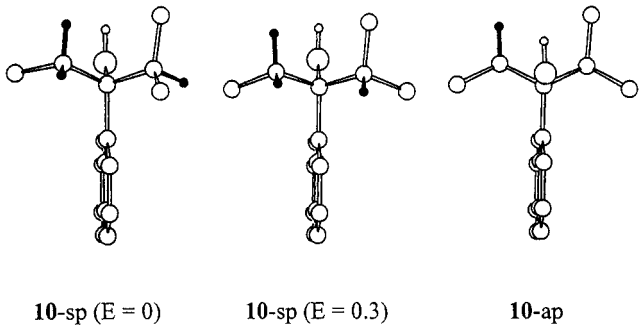


[a] The conformers differ by the relative position of the CH isopropyl hydrogen. That on the left ($E = 0$) is computed to be more stable by 0.3 kcal mol$^{-1}$ than that in the center. On the right is reported the most stable conformer of **10**-ap.

The same calculations, on the other hand, suggest that derivative **10** should be a good candidate for observing two stereolabile diastereoisomers (i.e., two conformers) since the two most stable rotational conformers of its **10**-sp atropisomer differ in the computed energy only by 0.3 kcal mol$^{-1}$ (their structures are reported in Chart 3). Furthermore, the calculations show that the two most stable conformers of **10**-sp differ indeed only by the position of the isopropyl and not by that of the ethyl moiety, as shown in Chart 3 where the $CH_2$ hydrogens (also indicated in black) occupy the same positions in the two conformers having $E = 0$ and 0.3 kcal mol$^{-1}$. These calculations also indicate that atropisomer **10**-ap should yield, on the contrary, the spectrum of a single conformer (Chart 3, right). This is because the two most stable conformers, differing by the position of the isopropyl group, have a computed energy separation as large as 3.4 kcal mol$^{-1}$.

The low-temperature NMR spectra of **10** (Figure 6) are in good agreement with such theoretical predictions. At −62 °C the signals of the two atropisomers become distinguishable, the major one (70%) having the ap structure (contrary to the case of **11** where the sp atropisomer was the more stable one). The interconversion barrier (Table 2) between **10**-ap and **10**-sp has a value ($\Delta G^{\ddagger} = 12.3$ kcal mol$^{-1}$) which is in between that of the more crowded diisopropyl derivative **2** and the less crowded diethyl derivative **3** (14.9 and 9.7 kcal mol$^{-1}$, respectively). This trend is analogous to that mentioned above for the case of **10** with respect to **2** and **4** (for the same reason the barrier of **10** is larger than that of the less hindered derivative **11**). At temperatures lower than −70 °C some of the $^{13}$C lines of the minor atropisomer **10**-sp (notably those corresponding to the CH of the isopropyl and the $CH_2$ and $CH_3$ of the ethyl moieties) broaden considerably and sharpen again on further cooling, a behavior typical for an exchange between two strongly biased species having a substantial chemical shift separation.[20] Careful inspection of the spectra taken at −135 °C (Figure 6) revealed the presence of a second conformer in about a 10% proportion. The $\Delta G°$ at this

(19) It has to be pointed out that the interpretation we offered for the apparent absence of dynamic processes in both **2**-ap and **3**-ap cannot be considered completely unambiguous. If one neglects the conclusions of the MM calculations and only relies upon the experimental findings, the existence of asymmetric (racemic) conformations also in **2**-ap and **3**-ap cannot be excluded in an absolute manner. In this event the absence of dynamic effects might be attributed to barriers too low to be detected by NMR. This is not totally unreasonable in view of the lower *tert*-butyl rotational barriers measured in **1**-ap with respect to **1**-sp.

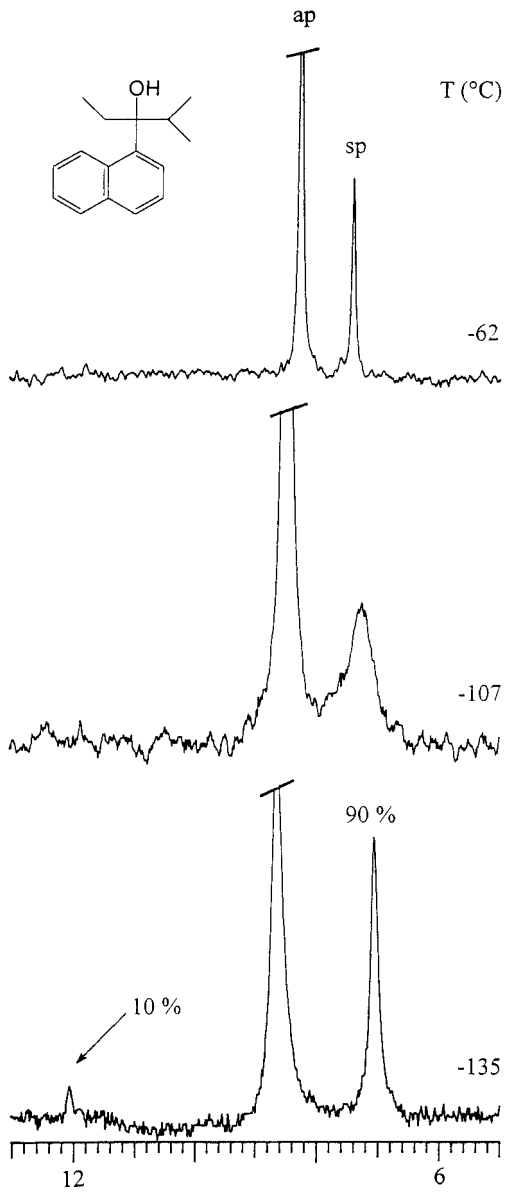


**Figure 6.** Methyl signals of the ethyl moiety of **10** ($^{13}$C NMR, 75.5 MHz) as a function of temperature in $Me_2O/CHF_2Cl/CD_3OD$ (1:1:1). Two sharp lines (ratio 7:3) due respectively to the major (**10**-ap) and the minor (**10**-sp) atropisomer are observed at −62 °C. The line of the latter (upfield) broadens on further lowering the temperature (the maximum line width being observed at −107 °C) and sharpens again, eventually displaying, at −135 °C, two signals (ratio 1:9) for the pair of conformers created by the restricted rotation of the isopropyl group (Chart 3).

temperature is 0.6 kcal mol$^{-1}$, which compares well with the computed energy difference of 0.3 kcal mol$^{-1}$ (Chart 3). The barrier for this dynamic process ($\Delta G^{\ddagger} = 7.6$ kcal mol$^{-1}$) is equal, within the errors (±0.2 kcal mol$^{-1}$), to that ($\Delta G^{\ddagger} = 7.2$ kcal mol$^{-1}$) for the dynamic process which exchanges the conformational enantiomers of **3**-sp by rotating the isopropyl groups.[21] We may thus conclude that in the atropisomer **10**-sp two different conformers, created by the restricted rotation along the Pr$^i$−COH stereogenic axis, have indeed been detected.

## Experimental Section

**Materials.** Naphthyldialkylmethanols **1**−**11** were prepared according to the following general procedure. To a cooled (−50 °C) solution of 1-naphthyllithium (15 mmol in 40 mL of anhydrous THF under $N_2$), obtained by halogen−metal exchange from 1-bromonaphthalene (15 mmol) and *n*-butyllithium (16 mmol, 1.6 M in hexane), the appropriate ketone (20 mmol in 5 mL of anhydrous THF) was added dropwise. After stirring (30 min) at −50 °C, the mixture was allowed to reach room temperature, and subsequently (1−20 h) the reaction was quenched with a saturated aqueous solution of $NH_4Cl$ and the mixture extracted with $Et_2O$. The organic layer was dried ($Na_2SO_4$) and concentrated *in vacuo*. Chromatography of the crude on silica gel or preparative thin-layer chromatography yielded the desired compounds.

**2,2,4,4-Tetramethyl-3-(1-naphthyl)pentan-3-ol, sp atropisomer (1-sp)**: $^1$H NMR ($CDCl_3$, 300 MHz) $\delta$ 1.16 (18H, s, C*Me*$_3$), 2.35 (1H, s, OH), 7.35−7.75 (6H, m, Ar), 9.50 (1H, m, H-8); $^{13}$C NMR ($CDCl_3$, 75.5 MHz) $\delta$ 30.0 ($CH_3$), 43.8 (C, *C*Me$_3$), 89.5 (C, COH), 122.5 (CH, Ar), 124.2 (CH, Ar), 125.0 (CH, Ar), 127.7 (CH, Ar), 128.0 (CH, Ar), 128.9 (CH, Ar), 129.1 (CH, Ar), 134.2 (C, Ar), 134.5 (C, Ar), 140.2 (C, Ar); MS *m*/*z* 270 (M$^+$). Anal. Calcd for $C_{19}H_{26}O$: C, 84.39; H, 9.69. Found: C, 84.48; H, 9.52.

**2,2,4,4-Tetramethyl-3-(1-naphthyl)pentan-3-ol, ap atropisomer (1-ap)**: mp 55−57 °C; $^1$H NMR ($CDCl_3$, 300 MHz) $\delta$ 1.20 (18H, s, C*Me*$_3$), 2.20 (1H, s, OH), 7.42−8.25 (6H, m, Ar), 8.60 (1H, m, H-8); $^{13}$C NMR ($CDCl_3$, 75.5 MHz) $\delta$ 31.0 ($CH_3$), 43.4 (C, *C*Me$_3$), 87.5 (C, COH), 123.6 (CH, Ar), 124.6 (CH, Ar), 125.5 (CH, Ar), 128.5 (CH, Ar), 128.8 (CH, Ar), 129.3 (CH, Ar), 130.4 (CH, Ar), 133.5 (C, Ar), 134.4 (C, Ar), 145.2 (C, Ar); MS *m*/*z* 270 (M$^+$). Anal. Calcd for $C_{19}H_{26}O$: C, 84.39; H, 9.69. Found: C, 84.53; H, 9.47.

**2,4-Dimethyl-3-(1-naphthyl)pentan-3-ol (2)**: $^1$H NMR ($CDCl_3$, 300 MHz) $\delta$ 0.95 (12H, bd, $CH_3$), 1.82 (1H, bs, OH), 2.65 (2H, bm, *CH*Me$_2$), 7.45−7.85 (6H, Ar), 9.47 (1H, bs, H-8); $^{13}$C NMR ($CDCl_3$, 75.5 MHz) $\delta$ 17.7 ($CH_3$), 35.7 (CH), 86.2 (C, COH), 124.2 (CH, Ar), 124.8 (CH, Ar), 125.1 (CH, Ar), 126.6 (CH, Ar), 128.2 (CH, Ar), 129.0 (CH, Ar), 129.1 (CH, Ar), 134.1 (C, Ar), 134.9 (C, Ar), 137.8 (C, Ar); MS *m*/*z* 242 (M$^+$). Anal. Calcd for $C_{17}H_{22}O$: C, 84.25; H, 9.15. Found: C, 84.40; H, 9.02.

**3-(1-Naphthyl)pentan-3-ol (3)**: $^1$H NMR ($CDCl_3$, 300 MHz) $\delta$ 0.78 (6H, t, $J_{AB}$ = 7.1 Hz, $CH_3$), 1.97 (1H, s, OH), 2.15 (2H, m, $J_{AB}$ = 7.1 Hz, $J_{gem}$ = 14.2 Hz, *CH*Me), 2.28 (2H, m, $J_{AB}$ = 7.1 Hz, $J_{gem}$ = 14.2 Hz, *CH*Me), 7.45−7.88 (6H, m, Ar), 8.84 (1H, m, H-8); $^{13}$C NMR ($CDCl_3$, 75.5 MHz) $\delta$ 8.2 ($CH_3$), 33.7 ($CH_2$), 79.1 (C, COH), 124.7 (CH, Ar), 124.9 (CH, Ar), 125.1 (CH, Ar), 126.3 (CH, Ar), 128.2 (CH, Ar), 129.3 (CH, Ar), 131.0 (C, Ar), 134.8 (C, Ar), 140.4 (C, Ar); MS *m*/*z* 214 (M$^+$). Anal. Calcd for $C_{15}H_{18}O$: C, 84.07; H, 8.47. Found: C, 84.31; H, 8.61.

**2-(1-Naphthyl)propan-2-ol (4)**: mp 94−96 °C; $^1$H NMR ($CDCl_3$, 300 MHz) $\delta$ 1.82 (6H, s, $CH_3$), 2.08 (1H, s, OH), 7.40−7.87 (6H, m, Ar), 8.84 (1H, dd, H-8); $^{13}$C NMR ($CDCl_3$, 75.5 MHz) $\delta$ 31.5 ($CH_3$), 74.1 (C, COH), 122.6 (CH, Ar), 124.7 (CH, Ar), 125.1 (CH, Ar), 125.2 (CH, Ar), 127.2 (CH, Ar), 128.6 (CH, Ar), 129.0 (CH, Ar), 130.9 (C, Ar), 134.8 (C, Ar), 143.3 (C, Ar); MS *m*/*z* 186 (M$^+$). Anal. Calcd for $C_{13}H_{14}O$: C, 83.82; H, 7.58. Found: C, 83.65; H, 7.69.

**2,4-Dimethyl-3-(2-methyl-1-naphthyl)pentan-3-ol (5), major atropisomer**: $^1$H NMR ($CDCl_3$, 300 MHz) $\delta$ 0.58 (6H, d, $CH_3$), 1.20 (6H, d, $CH_3$), 1.90 (1H, s, OH), 2.80 (3H, s, Ar-*CH*$_3$), 2.98 (2H, m, *CH*-Me$_2$), 7.34−7.73 (5H, m, Ar), 8.19 (1H, m, H-8); $^{13}$C NMR ($Me_2O/C_6D_6$, −30 °C, 75.5 MHz) $\delta$ 18.7 ($CH_3$), 19.7 ($CH_3$), 26.1 (Ar-*CH*$_3$), 37.7 (CH), 84.9 (C, COH), 123.8 (CH, Ar), 124.3 (CH, Ar), 126.6 (CH, Ar), 126.9 (CH, Ar), 129.0 (CH, Ar), 132.0 (CH, Ar), 132.7 (C, Ar), 133.8 (C, Ar), 135.5 (C, Ar), 142.2 (C, Ar); MS *m*/*z* 256 (M$^+$). Anal. Calcd for $C_{18}H_{24}O$: C, 84.32; H, 9.44. Found: C, 84.54; H, 9.52.

**2,4-Dimethyl-3-(2-methyl-1-naphthyl)pentan-3-ol (5), minor atropisomer**: $^1$H NMR ($CDCl_3$, 300 MHz) $\delta$ 0.78 (6H,

(20) Anet, F. A. L.; Basus, V. J. *J. Magn. Reson.* **1978**, *32*, 339. See also: Sandström, J. *Dynamic NMR Spectroscopy*; Academic Press: London, 1982; p 84.

(21) The rotation of the ethyl group is expected to be too fast to be NMR detectable at −135 °C, as one can infer from the quite low rotational barrier (observed below −140 °C) for the ethyl group in **3**-sp (i.e., 6.1 kcal mol$^{-1}$). Unfortunately at temperatures lower than −135 °C compound **10** becomes insoluble.

d, $CH_3$), 1.20 (6H, d, $CH_3$), 2.10 (1H, s, OH), 2.62 (3H, s, Ar-*$CH_3$*), 2.80 (2H, m, *CH*-$Me_2$), 7.34−7.73 (5H, m, Ar), 9.26 (1H, m, H-8); $^{13}$C NMR ($Me_2O/C_6D_6$, −30 °C, 75.5 MHz) $\delta$ 18.6 ($CH_3$), 19.5 ($CH_3$), 25.6 (Ar-*$CH_3$*), 36.7 (CH), 84.9 (C, COH).

**3-(2-Methyl-1-naphthyl)pentan-3-ol (6)**: $^1$H NMR ($CDCl_3$, 300 MHz) $\delta$ 0.83 (6H, t, $CH_3$), 1.88 (1H, s, OH), 2.02 (2H, m *CH*Me), 2.55 (4H, m, *CH*Me), 2.74 (3H, s, Ar-*$CH_3$*), 7.20−7.73 (5H, m, Ar), 8.56 (1H, m, H-8); $^{13}$C NMR ($CD_2Cl_2$, 75.5 MHz) $\delta$ 8.5 ($CH_3$), 25.8 (Ar-*$CH_3$*), 35.9 ($CH_2$), 82.6 (C, COH), 124.4 (CH, Ar), 124.9 (CH, Ar), 127.0 (CH, Ar), 127.7 (CH, Ar), 129.0 (CH, Ar), 132.4 (CH, Ar), 132.6 (C, Ar), 134.0 (C, Ar), 135.4 (C, Ar), 138.8 (C, Ar); MS *m/z* 228 ($M^+$). Anal. Calcd for $C_{16}H_{20}O$: C, 84.16; H, 8.83. Found: C, 84.02; H, 8.52.

**2-(2-Methyl-1-naphthyl)propan-2-ol (7)**: $^1$H NMR ($CDCl_3$, 300 MHz) $\delta$ 1.86 (1H, s, OH), 1.95 (6H, s, $CH_3$), 2.68 (3H, s, Ar-*$CH_3$*), 7.19−7.75 (5H, m, Ar), 8.71 (1H, m, H-8); $^{13}$C NMR ($CD_2Cl_2/Me_2O$, −15 °C, 75.5 MHz) $\delta$ 25.4 (Ar-*$CH_3$*), 32.3 ($CH_3$), 75.3 (C, COH), 124.1 (CH, Ar), 124.2 (CH, Ar), 127.3 (CH, Ar), 128.4 (CH, Ar), 128.5 (CH, Ar), 131.8 (CH, Ar), 132.7 (C, Ar), 134.0 (C, Ar), 134.1 (C, Ar), 142.9 (C, Ar); MS *m/z* 200 ($M^+$). Anal. Calcd for $C_{14}H_{16}O$: C, 83.96; H, 8.05. Found: C, 84.09; H, 8.22.

**3,3-Dimethyl-2-(1-naphthyl)butan-2-ol (8)**: $^1$H NMR ($CDCl_3$, 300 MHz) $\delta$ 1.08 (9H, s, C*$Me_3$*), 1.85 (3H, s, $CH_3$), 1.98 (1H, s, OH), 7.35−7.90 (6H, m, Ar), 9.36 (1H, m, H-8); $^{13}$C NMR ($CDCl_3$, 75.5 MHz) $\delta$ 26.8 ($CH_3$, C*$Me_3$*), 29.4 ($CH_3$), 39.7 (C, *C*$Me_3$), 83.7 (C, COH), 123.9 (CH, Ar), 124.7 (CH, Ar), 124.8 (CH, Ar), 127.9 (CH, Ar), 128.4 (CH, Ar), 128.7 (CH, Ar), 129.8 (CH, Ar), 133.2 (C, Ar), 134.7 (C, Ar), 141.5 (C, Ar); MS *m/z* 228 ($M^+$). Anal. Calcd for $C_{16}H_{20}O$: C, 84.16; H, 8.83. Found: C, 84.01; H, 8.69.

**3,3-Dimethyl-2-(2-naphthyl)butan-2-ol (9) (obtained as a secondary product from 8)**: $^1$H NMR ($CDCl_3$, 300 MHz) $\delta$ 1.02 (9H, s, C*$Me_3$*), 1.73 (3H, s, $CH_3$), 1.81 (1H, s, OH), 7.41−7.96 (7H, m, Ar); $^{13}$C NMR ($CDCl_3$, 75.5 MHz) $\delta$ 25.4 ($CH_3$), 25.8 ($CH_3$, C*$Me_3$*), 38.3 (C, *C*$Me_3$), 78.7 (C, COH), 125.6 (CH, Ar), 125.7 (CH, Ar), 125.8 (CH, Ar), 125.9 (CH, Ar), 126.3 (CH, Ar), 127.3 (CH, Ar), 128.2 (CH, Ar), 132.0 (C, Ar), 132.3 (C, Ar), 143.8 (C, Ar); MS *m/z* 228 ($M^+$). Anal. Calcd for $C_{16}H_{20}O$: C, 84.16; H, 8.83. Found: C, 84.05; H, 8.95.

**2-Methyl-3-(1-naphthyl)pentan-3-ol (10)**: $^1$H NMR ($CDCl_3$, 300 MHz) $\delta$ 0.62 (3H, bt, $J$ = 7.4 Hz, $CH_2CH_3$), 0.71 (3H, bd, $J$ = 6.8 Hz, $CHCH_3$), 1.05 (3H, bd, $J$ = 6.8 Hz, $CHCH_3$), 1.84 (1H, bs, OH), 2.05 (1H, m, $J_{gem}$ = 14.8 Hz, $J_{AB}$ = 7.4Hz, *CH*Me), 2.40 (1H, m, $J_{gem}$ = 14.8 Hz, $J_{AB}$ = 7.4 Hz, *CH*Me), 2.62 (1H, sept, $J$ = 6.8 Hz, *CH*$Me_2$), 7.36−7.86 (6H, m, Ar), 8.54 (1H, bs, H-8); $^{13}$C NMR ($CDCl_3$, 75.5 MHz) $\delta$ 8.3 ($CH_3$), 16.9 ($CH_3$), 17.5 ($CH_3$), 30.8 ($CH_2$), 36.1 (CH), 81.0 (C, COH), 124.7 (CH, Ar), 124.8 (CH, Ar), 125.0 (CH, Ar), 125.6 (CH, Ar), 128.0 (CH, Ar), 129.4 (CH, Ar), 130.9 (C, Ar), 134.9 (C, Ar), 140.7 (C, Ar); MS *m/z* 228 ($M^+$). Anal. Calcd for $C_{16}H_{20}O$: C, 84.16; H, 8.83. Found: C, 83.95; H, 8.62.

**3-Methyl-2-(1-naphthyl)butan-2-ol (11)**: mp 45−46 °C; $^1$H NMR ($CDCl_3$, 300 MHz) $\delta$ 0.75 (3H, d, $J$ = 7.5 Hz, *$CH_3$*-CH), 0.95 (3H, d, $J$ = 7.5 Hz, *$CH_3$*CH), 1.70 (3H, s, $CH_3$), 1.96 (1H, bs, OH), 2.77 (1H, sept, $J$ = 7.5 Hz, *CH*$Me_2$), 7.32−7.86 (6H, m, Ar), 8.70−8.80 (1H, m, H-8); $^{13}$C NMR ($CDCl_3$, 75.5 MHz) $\delta$ 17.0 ($CH_3$), 18.2 ($CH_3$), 25.1 ($CH_3$), 36.1 (CH), 78.9 (C, COH), 124.2 (CH, Ar), 124.5 (CH, Ar), 124.9 (CH, Ar), 127.1 (CH, Ar), 128.3 (CH, Ar), 129.1 (CH, Ar), 130.8 (C, Ar), 135.0 (C, Ar), 143.2 (C, Ar); MS *m/z* 214 ($M^+$). Anal. Calcd for $C_{15}H_{18}O$: C, 84.07; H, 8.47. Found: C, 83.94; H, 8.63.

**NMR Measurements.** The variable temperature NMR spectra were recorded at 300 MHz ($^1$H) and 75.5 MHz ($^{13}$C). The computer simulation of the line shape was performed by a computer program[22] based on the Bloch equations, and the best fit was visually judged by superimposing the plotted and experimental traces. The samples for measurements below −100 °C were prepared by connecting the NMR tubes, containing a small amount of a deuterated compound for locking purpose, to a vacuum line and condensing the gaseous solvents ($Me_2O$ or $CHF_2Cl$) with liquid nitrogen. The tubes were then sealed *in vacuo* and introduced in the precooled probe of the spectrometer. The difference NOE measurements were carried out in solutions purged from dissolved oxygen, using a nitrogen stream, by presaturating the signal for about 10 s and acquiring the spectrum with the decoupler turned off. The various lines of the multiplets were saturated by cycling the irradiation frequencies about 40 times. A program which accumulates the difference between the two FIDs (that being irradiated and that acquired with the irradiation frequency kept away from any signal) was employed. The control spectrum was subsequently acquired with one-half the number of scans.

**Acknowledgment.** The authors thank Dr. F. Bologna for skillful assistance. This work was carried out with the financial support of the National Research Council (CNR) and of the Ministry the University and Scientific Research (MURST), Rome.

JO970113+

(22) (a) Casarini, D.; Lunazzi, L.; Macciantelli, D. *J. Chem. Soc. Perkin Trans. 2* **1985**, 1839. (b) Bonini, B. F.; Grossi, L.; Lunazzi, L.; Macciantelli, D. *J. Org. Chem.* **1986**, *51*, 517.